

EGF stimulates lamellipod extension in metastatic mammary adenocarcinoma cells by an actin-dependent mechanism

Jeffrey E. Segall, Sangeeta Tyerech*, Lucia Boselli*, Susan Masseling, Joseph Helft, Amanda Chan, Joan Jones† and John Condeelis

Departments of Anatomy and Structural Biology, *Radiation Oncology, and †Pathology, Albert Einstein College of Medicine, Bronx, NY, USA

(Received 11 July 1995; accepted in revised form 24 September 1995)

Changes in lamellipod extension and chemotaxis in response to EGF were analysed for MTLn3 cells (a metastatic cell line derived from the 13762NF rat mammary adenocarcinoma). Addition of EGF produced a cessation of ruffling followed by extension of hyaline lamellipods containing increased amounts of F-actin at the growing edge. A non-metastatic cell line (MTC) derived from the same tumor did not show such responses. Lamellipod extension was maximal within 5 min, followed by retraction and resumption of ruffling. Maximal area increases due to lamellipod extension occurred at about 5 nM EGF. Chemotactic and chemokinetic responses, measured using a microchemotaxis chamber, were also greatest at 5 nM. Cytochalasin D inhibited EGF-stimulated responses including lamellipod extension, increases in F-actin in lamellipods, and chemotaxis. Nocodazole affected chemotaxis at higher concentrations but not EGF-induced lamellipod extension. We conclude that polymerization of F-actin at the leading edges of lamellipods is necessary for extension of lamellipods and chemotaxis of MTLn3 cells in response to EGF. The motility and chemotaxis responses of this metastatic cell line have strong similarities to those seen in well-characterized chemotactic cells such as *Dictyostelium* and neutrophils.

Keywords: chemotaxis, EGF, metastasis, motility

Introduction

Metastasis, the seeding of distant sites by a malignant tumor, is a major cause of morbidity and mortality in cancer patients [1–3]. The process, however, is complex, and dependent upon successful completion of a number of sequential events [4–9]. As outlined in the 3-step hypothesis of invasion, tumor cells must form attachments to extracellular matrix, degrade the matrix, and migrate [10]. Following a series of these occurrences, cells may enter lymphatic or vascular channels, and repetition of the same process of attachment, degradation, and migration at a distant

site will lead to establishment of a metastasis. A key feature, then, of metastasis is migration, i.e. cell motility and chemotaxis.

The motility and chemotaxis of amoeboid cells has been most extensively characterized in non-metastatic cells such as *Dictyostelium* and neutrophils (for reviews, see [11–13]). One of the consequences of chemoattractant exposure is the stimulation of actin polymerization and pseudopod formation. In a spatial gradient, the cells move towards higher concentrations of chemoattractant. A number of methods have been developed for the analysis of cell behavior, including the Boyden chamber (and modifications thereof) and video analysis of cell shape changes in response to rapid upshifts in chemoattractant concentration. The results from such studies have indicated that one of the responses to chemoattractants

Address correspondence to: J. E. Segall, Department of Anatomy and Structural Biology, Albert Einstein College of Medicine, 1300 Morris Park Avenue, Bronx, NY 10461, USA. Tel (+1) 718 430 4237; Fax: (+1) 718 430 8996, Email: segall@acom.yu.edu.

is the extension of actin-filled pseudopods. Numerous biochemical and genetic studies have identified proteins that are important for cell motility and chemotaxis in these cells. Do these proteins play homologous roles in metastatic cell motility? Are they critical for the ability of tumor cells to metastasize?

To answer these questions, it is first necessary to determine if the motility and chemotaxis responses of metastatic cells are similar to those of amoeboid phagocytes. A number of motility factors for tumor cells have been identified. Autocrine motility factors [14,15] are thought to act through G-protein coupled receptors, as do many of the chemoattractants for phagocytes. However, in mesenchymal and epithelially derived cells, growth factors acting through receptor tyrosine kinases (such as EGF [16–21], PDGF [22], insulin [23], and HGF/SF [24,25]) can also act as chemoattractants. Such responses may be clinically relevant. For example, overexpression of the EGF receptor has been found to correlate with a poorer prognosis for certain cancer patients [26–31].

Analysis of EGF-stimulated signal transduction has benefited from studies utilizing the A431 carcinoma cell line [32–35]. Although extremely useful for studies of signal transduction, A431 cells are not highly metastatic [36]. MTLn3 cells are clonally derived from a lung metastasis from the 13762NF rat mammary adenocarcinoma [37]. Upon injection of MTLn3 cells into the rat mammary fat pad (a spontaneous metastasis assay), a primary tumor forms followed by widespread lung and lymph node metastases at high frequency [38]. This metastatic potential remains for a large number of passages [39]. The cell surface receptors for EGF have been characterized for these cells [40,41]. Thus the MTLn3 cell line provides a convenient model system for the study of breast cancer cells and metastasis.

The purpose of the work reported in this paper was to examine in detail the chemotactic and motile responses of MTLn3 cells to EGF. By analysing the relationship between actin polymerization and rapid changes in cell shape and chemotactic responses, we conclude that actin polymerization at the leading edge of the lamellipodium plays an important role in stimulation of lamellipod extension and chemotaxis of MTLn3 cells.

Materials and methods

Cell lines and culture conditions

The cell lines used in this study are the MTLn3 and MTC lines. The MTLn3 line was derived as a single cell clone from a lung metastasis of the 13762NF rat

mammary adenocarcinoma, while the non-metastatic MTC line was derived as a single cell clone from the parental tumor [37] (both kindly provided by Dr G. Nicolson, MD Anderson Cancer Center, Houston, TX, USA). Cells were frozen in liquid nitrogen at passages 15–17, and used until passage 25. They were grown in alpha-modified MEM containing L-glutamine (Gibco 12561-031) supplemented with 5% FCS (Sigma 4884) and antibiotics (Sigma P0906). At 60–80% confluence, cells were harvested for passaging and for experiments by removing medium, rinsing with trypsin/EDTA (Gibco 25300-062), incubating at 37°C for 2–4 min, then stopping with whole medium, and diluting in whole medium to the desired density.

Lamellipod extension assay

Tissue culture dishes, Nucleopore filters, or glass coverslips were coated with 27 µg/ml rat tail collagen I (Collaborative Biochemicals no. 40236) in DPBS without calcium or magnesium (JRH Biosciences) for 2 h. The collagen solution was aspirated and replaced with complete growth medium containing 12 mM HEPES, pH 7.4 (termed MEMH). Cells were harvested and plated at a density of 6250 cells/cm². The dishes were incubated for 20–24 h in a tissue culture incubator and were then covered with mineral oil (Sigma 400-5) to block evaporative cooling during the experiment [42]. (Mineral oil had no observable effects upon the responses studied here.) The dishes were viewed with a Nikon Diaphot microscope in a Nikon temperature chamber at 37°C. Additions to the medium were made with a pump using prewarmed tubing such that additions took about 30 s. Efficient mixing was ensured by adding a volume equal to the volume already in the dish. Trial experiments using dyes indicated mixing was complete within 1 min.

For most experiments, the cells were viewed with a 10× phase objective, and the images were recorded both on videotape and directly on a Macintosh Quadra. Typically, an image was stored on the computer every minute, forming a movie using the program NIH Image. For analysis, the movies were analysed using 2-D DIAS (Solltech, Iowa City, IA, USA [43]), to provide measurements of the area for each cell. The area for each cell was then divided by its area before stimulation to give a normalized area at each time point. Then the normalized areas for each time point were averaged.

For treatments with cytochalasin D or nocodazole (Sigma), the drugs were dissolved in DMSO, and then diluted into MEMH to the appropriate concentration. The final concentration of DMSO ranged from 0.1 to 0.4%, and control stimulation with MEMH alone

always contained the same concentration of DMSO as that used in the drug treatment. The cells were first exposed to medium containing drug or DMSO at the indicated concentration for 1 min. This was followed by addition of medium containing drug and EGF or DMSO and EGF; lamellipod extension was quantified at 4 min after addition of EGF. Exposure to drug alone during this time had no effect on cell area. Studies with nocodazole showed that longer exposure to drug before stimulation with EGF produced similar results.

Microchemotaxis chamber studies

For the analysis of chemotactic responses, a 48-well microchemotaxis chamber (Neuroprobe, Cabin John, MD, USA) was utilized, essentially following the manufacturer's instructions. A Nucleopore filter with 8 μm pores was coated with collagen I for 2 h as described above. The lower wells of the chamber were filled with MEMH containing the appropriate compounds; then the chamber was assembled. The upper wells were then filled with MEMH containing 15 000 cells. The wells were incubated at 37°C for 3 h, then disassembled, and the upper side of the filter scraped to remove cells that had not travelled through the filter. The filters were then fixed in 3.7% formaldehyde in PBS, washed twice in water, and then stained for 12–18 h in hematoxylin. The filters were then rinsed in water and mounted for viewing. All the nuclei of the cells in each well that crossed the filter were counted.

F-actin staining

Ethanol-rinsed coverslips were sterilized with UV light and coated with collagen I as described above. Cells were plated onto the coverslips in MEMH and incubated for 20–24 h in a Petri dish. Stimulation was followed at selected time points by aspiration of medium, and fixation for 5 min in 3.7% formaldehyde in PBS (137 mM NaCl, 5 mM KCl, 1.1 mM Na₂HPO₄, 0.4 mM KH₂PO₄, 4 mM NaHCO₃, 5.5 mM glucose, 2 mM MgCl₂, 2 mM EGTA, 5 mM Pipes, pH 7.2), at 37°C. Further steps were performed at room temperature. The fix solution was aspirated and 0.5% Triton X-100 in PBS applied for 20 min. This was then washed once and replaced with 0.1 M glycine in PBS for 10 min. The cells were then washed five times with PBS. The solution was aspirated and then the cells were stained with 1 μM rhodamine phalloidin for 20 min in a humidified chamber. After five washes with PBS, the coverslips were mounted in 0.1 M N-propyl gallate, 0.02% NaN₃, in 50% glycerol in PBS, pH 7.0.

Rhodamine-phalloidin localization was performed using a N.A. 1.4 60 \times objective on either a BioRad

MRC-600 confocal microscope or a Nikon Diaphot with fluorescence optics. Data collected on the confocal microscope were accumulated as a z-series with a 0.39 μm pixel dimension. For quantitation of total fluorescence and fluorescence as a function of distance from the edge of the lamellipod, data were collected using a SIT camera (Hamamatsu) on the Diaphot. For each data collection session, the gain and offset of the camera were adjusted so that <0.01% of the pixels were saturated. The same settings were then used to collect data from cells at each of the experimental conditions being tested. At each collection session, data for equal numbers of cells from each experimental condition were collected. The output of the SIT camera was collected on a Macintosh computer using NIH Image. Each image was averaged, then stored, together with a phase contrast image of the cell. For analysis, hyaline lamellipods of the cell periphery lacking ruffles were identified. A line was drawn along the cell border in that region, and a macro utilized to calculate the mean fluorescence intensity along the border, and then the mean value for successive lines moving into the cell in 1 pixel steps. The result was a curve of the mean fluorescence in hyaline lamellipods as a function of the distance from the border of the lamellipod. Curves for all cells under a particular stimulus condition were averaged to produce the mean fluorescence profile in lamellipods for that condition. To measure average whole cell fluorescence, the average pixel intensity of all the values of all the pixels within the cell were averaged. This was then multiplied by the total cell area to give total cell fluorescence.

Quantitation of F-actin content was performed with the NBD-phalloidin assay as described previously [44] with the following modifications. Cells (2×10^5) were plated in each 35 mm Petri dish. Cells were stimulated with EGF or with buffer controls and fixed as described above. Cells were washed with multiple changes of PBS for 45 min and stained with 0.5 ml of 0.2 μM NBD-phalloidin (Molecular Probes) for 1 h. Cells were washed twice in PBS and extracted with 0.5 ml of 100% methanol for 90 min. Fluorescence of the extraction solution was recorded at 465 nm excitation and 535 nm emission.

Results

Preliminary studies indicated that in the absence of serum, MTLn3 cells were unable to attach and spread on laminin, fibronectin, collagen I or collagen IV. In the presence of at least 0.5% serum, some attachment and spreading was observed. At low serum concentra-

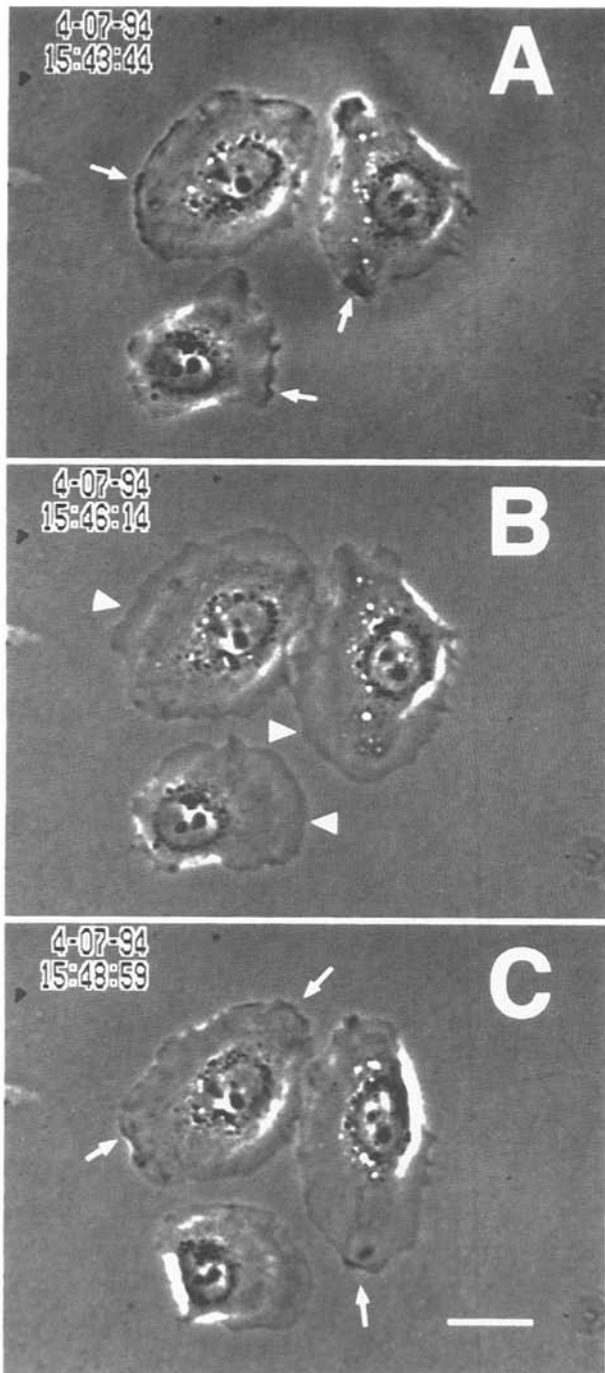


Figure 1. Lamellipod extension occurs in response to EGF. Cells were viewed with a $\times 40$ objective before and after stimulation with 5 nM EGF. (A) Before, (B) 3 min after, and (C) 5.5 min after addition of EGF. Ruffles are indicated by arrows in (A) and (C), and areas of lamellipod extension are indicated by arrowheads in (B). Bar = 20 μ m.

tions, collagen I appeared to provide the best substratum for attachment and spreading. This is consistent with other studies indicating that MTLn3 cells are more adherent to collagen than fibronectin

[40]. Therefore, all further experiments utilized surfaces coated with collagen I.

Cells plated on collagen and then stimulated with EGF showed a biphasic response. Initially, ruffling ceased and a flat, thin lamellipodium spread out along the substratum (Figure 1). Extension of the lamellipod resulted in an increase in the surface area covered by each cell. After 3–4 min, ruffling began and the lamellipodium slowly retracted. Comparison of the responses of MTLn3 cells stimulated with EGF, bFGF, PDGF, insulin, IGF-1, or MSH indicated that the strongest response was induced by EGF (data not shown). More detailed analysis of the kinetics of the response to EGF (Figure 2) was performed using 2-D DIAS software, quantitating lamellipod extension as increases in cell area. The area began to increase within 1 min after addition of EGF. For 5 nM EGF (Figure 2B), the area was maximal about 4 min after stimulation, increasing by about 27% over prestimulus values. It then decreased over the next 5–6 min, but did not return to baseline, remaining about 8% above prestimulus values. Similar responses were observed using TGF α as stimulus (data not shown).

Lamellipod extension was measured as a function of EGF concentration (Figure 3). Buffer alone produced a slight retraction of cell extensions. Area increases were clear at 0.2 nM and had saturated by 25 nM. The maximal change in area showed a sigmoidal dependence on EGF concentration, with an estimated K_{50} of about 0.5 nM. Binding of EGF to MTLn3 cells has revealed two receptors, with K_d values of 0.17 and 1.2 nM [40,41]. Thus lamellipod extension could reflect binding to either or both of these receptor classes.

We also tested the responses of a non-metastatic cell line derived from the same original tumor. The MTC cells can form a primary tumor when injected into the mammary fat pad, but do not metastasize to lymph nodes or lungs [38]. They show markedly reduced levels of EGF binding [40]. These cells show little response to EGF (data not shown) or TGF α (Figure 4). This supports the interpretation that the responses reported here are mediated by the EGF receptor.

Rapid, transient expansions of lamellipods or pseudopods in response to a specific compound could reflect chemotactic responses. For example, stimulation of *Dictyostelium* cells or neutrophils with the chemoattractants cAMP or F-MetLeuPhe, respectively, leads to such responses. Therefore, a 48-well microchemotaxis chamber was used to determine if EGF was a chemoattractant for MTLn3 cells. With a gradient of EGF, there was a significant increase in the number of cells crossing the filter, with the

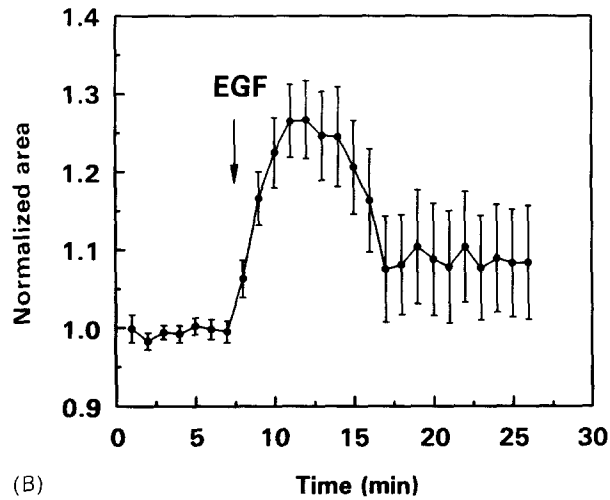
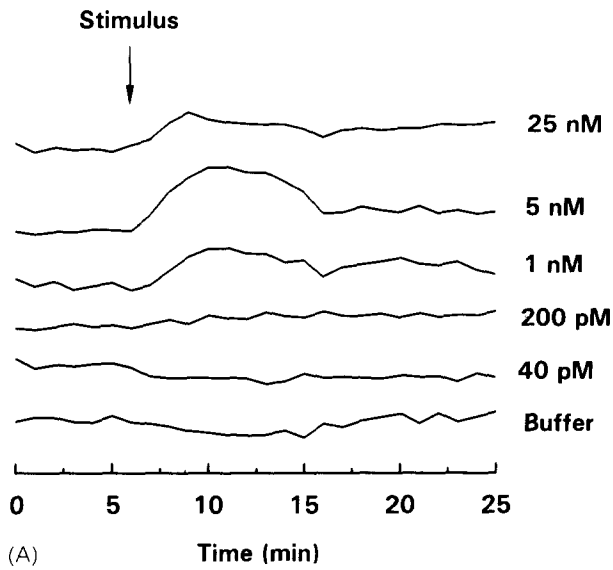


Figure 2. Kinetics of lamellipod extension in response to EGF. Lamellipod extension was quantitated as increases in cell area. (A) Cells were followed for 7 min before stimulation and then EGF was added between minutes 7 and 8 at the dose indicated. (B) Kinetics of the area increase at the optimum dose of 5 nM. The area at each data point for each cell is normalized to the mean area of the cell before stimulation. Then the normalized values at each time point were averaged and a standard error of the mean calculated. Data from 26 cells from three separate experiments were averaged.

maximal response at about 5 nM (Figure 5, filled symbols). Chemotactic responses should require a gradient in concentration of the chemoattractant. By placing equal concentrations of EGF on both sides of the filter, the degree of random motility stimulated by EGF (chemokinesis) can be estimated (Figure 5, open symbols). By this criterion, the chemokinetic response to EGF is roughly one-half the response produced by

a gradient, indicating that the remaining response must reflect the response to the gradient, or chemotaxis. Thus, EGF stimulates both chemotactic and chemokinetic responses in MTLn3 cells.

A number of studies have indicated that actin

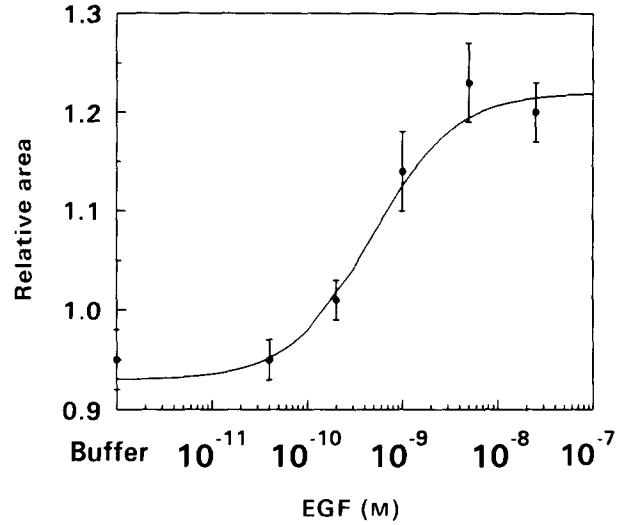


Figure 3. Sensitivity of lamellipod extension to EGF. The areas of cells relative to the prestimulus areas were determined at 3 min after stimulation with EGF. The normalized value for each cell was then averaged with other cells exposed to the same EGF concentration to produce a mean and SEM. Each data point represents the average of 18–30 cells from three separate experiments. The data were fitted to a curve of the form $C/(C + K_d)$, with a best fit K_d of 0.5 nM.

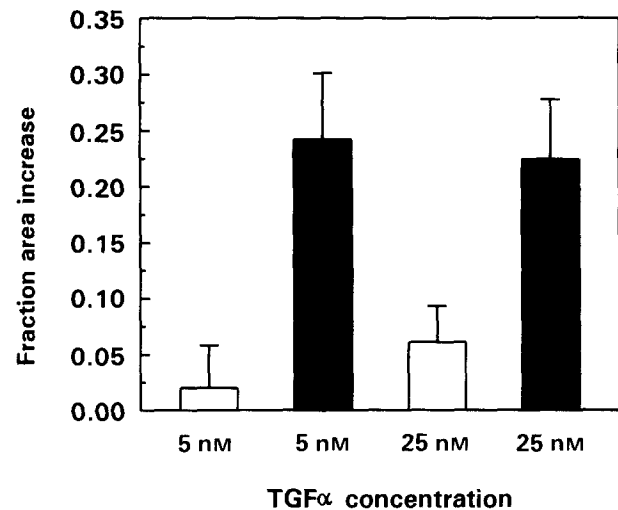


Figure 4. Comparison of responses of MTC and MTLn3 cells to TGF α . MTC cells (open bars) or MTLn3 cells (filled bars) were stimulated with the concentrations of TGF α shown, and the area change 4 min after stimulation was measured. Results are the mean and SEM of 20 cells from two separate experiments.

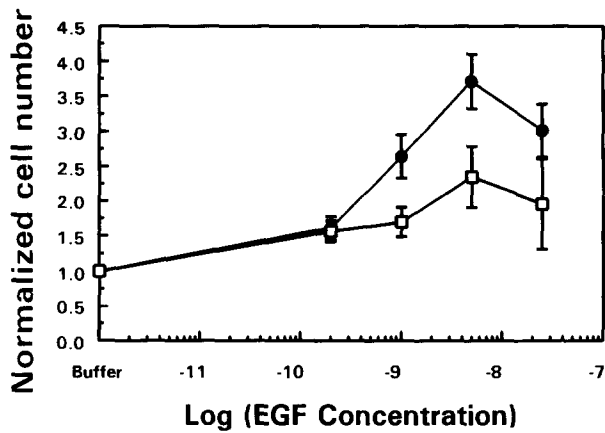


Figure 5. Migration of MTLn3 cells in response to EGF. For each experiment, the number of cells crossing the filter in 3 h was normalized to the number crossing in the absence of EGF (average value 70). These normalized values were then averaged to produce ensemble means and SEM for a total of 12 wells in three separate experiments. ● = EGF present only in the bottom well (generating a spatial gradient to measure chemotaxis). □ = EGF present in both the top and bottom wells (isotropic conditions to measure chemokinesis).

polymerization accompanies extension of lamellipods and pseudopods. The total amount of F-actin, measured as total binding of phalloidin to permeabilized cells, did not show any significant change in response to stimulation by EGF. Resting levels of F-actin were 167.8 ± 7.3 compared to 181.2 ± 10.6 or 182.3 ± 8.2 for cells stimulated with medium alone or medium containing EGF, respectively (mean and SEM of 19 experiments in arbitrary units, with *t*-tests showing no significant differences). However, localization studies using rhodamine-phalloidin revealed a clear difference between EGF-stimulated and buffer-stimulated cells (Figure 6). At the leading edges of newly formed lamellipods (the sites of cell spreading), there is an increase in rhodamine-phalloidin labelling, indicating an increase in the amount of F-actin in areas of cell expansion. When quantified as a function of distance from the edge of the cell, hyaline regions of the cell periphery showed more staining near the edge of the cell in EGF-stimulated cells (Figure 7, filled circles), as compared to cells stimulated with medium alone (Figure 7, filled squares).

Does the increased F-actin at the edge of growing lamellipods play a function in the growth of the lamellipods or occur in response to the sudden expansion of lamellipods? To determine if actin polymerization is necessary for pseudopod expansion, we measured the responses of cells in the presence of cytochalasin D, a compound that blocks actin polymerization by binding to the growing ends of

actin filaments [45]. Preliminary experiments indicated that MTLn3 cells are extremely sensitive to the presence of cytochalasin D. Application of 100 nM cytochalasin D leads to the arrest of lamellipod formation and cell rounding, even in the absence of EGF. By using lower concentrations of cytochalasin and brief exposure times (1–5 min), it was possible to stimulate cells with EGF before there was significant rounding up. Cytochalasin D (50 nM) inhibited increases in area and lamellipod extension due to EGF by about 60% (Figure 8). This concentration of cytochalasin D also inhibited the increase in F-actin that occurs in lamellipods in response to EGF (Figure 7, open symbols). Indeed, cytochalasin D caused a significant decrease in the F-actin content of both lamellipods and whole cells after EGF stimulation (Figure 7 and Table 1). This indicates that EGF addition stimulates both polymerization and depolymerization of F-actin in cells. Cytochalasin D then blocks the stimulated polymerization by binding

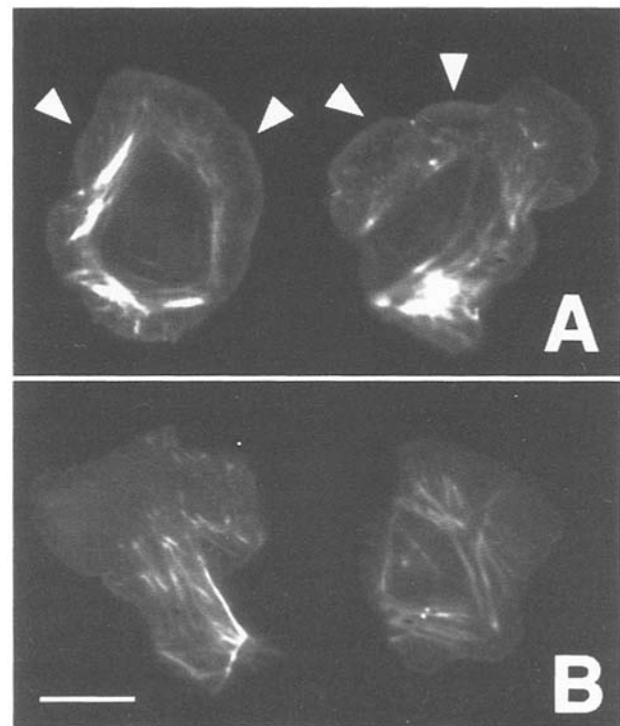


Figure 6. Localization of F-actin. Cells were stimulated with 5 nM EGF (A) or MEMH (B), fixed 3 min after stimulation, and stained with rhodamine phalloidin as described in Materials and methods. The cells were then viewed with a SIT camera. Two different cells from each stimulus condition are shown. All images were collected and displayed at identical settings to allow direct comparison. Arrowheads indicate areas of increased F-actin at the leading edges of extending lamellipods in EGF-stimulated cells. Bar = 10 μ m.

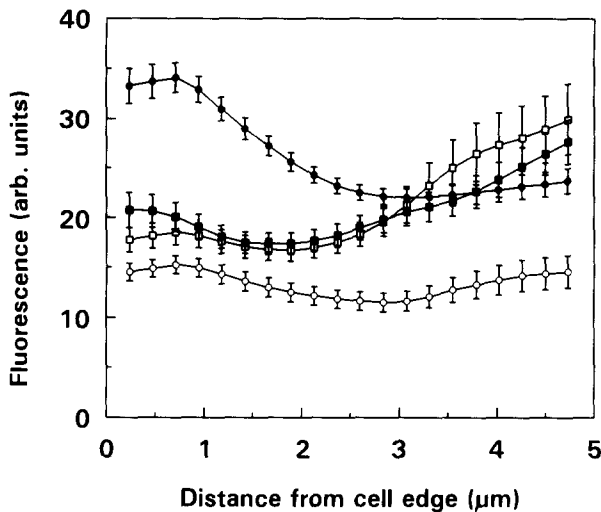


Figure 7. Distribution of rhodamine phalloidin staining in hyaline lamellipods 3 min after EGF stimulation. The rhodamine-phalloidin fluorescence was quantitated as a function of distance from the edge of the lamellipod, as described in Materials and methods. ●, Cells stimulated with 5 nM EGF; ■, cells stimulated with MEMH; ○, cells exposed to 50 nM cytochalasin D for 1 min before stimulation with 5 nM EGF; □, cells exposed to 50 nM cytochalasin D for 1 min before stimulation with MEMH. Data are the means and SEM for 12–15 cells.

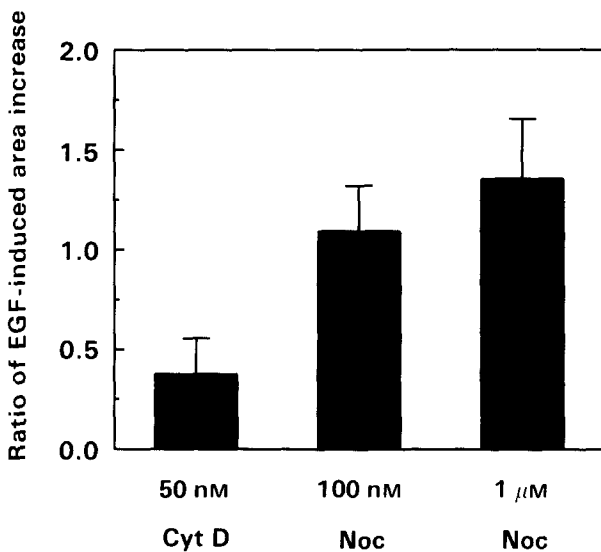


Figure 8. Effects of cytoskeletal inhibitors on EGF-induced lamellipod extension. Cells were stimulated with EGF in the presence or absence of the indicated inhibitor concentrations. Areas at 4 min were normalized to prestimulus values and averaged to yield means and SEM.

to the barbed end of growing actin filaments, but does not block depolymerization occurring presumably from pointed filament ends.

The high sensitivity of both the EGF-induced

lamellipodial growth and local increases in F-actin to cytochalasin D suggests that actin polymerization at the growing lamellipod is important for lamellipod expansion and chemotaxis. This was supported by studies using the microchemotaxis chamber. The number of cells crossing the filter in response to a gradient of EGF was reduced by 50% in 1–10 nM cytochalasin D (Figure 9). The greater sensitivity to cytochalasin D in the microchemotaxis assay may

Table 1. Cytochalasin D effects on total cellular F-actin

Condition	Total fluorescence/cell (arbitrary units)	SEM
Medium	1.74	0.12
EGF (5 nM)	1.92	0.15
Medium + cyto D	1.89	0.24
EGF (5 nM) + cyto D	0.77	0.07

Cells were preincubated with medium alone or 50 nM cytochalasin D, then stimulated with medium alone or 5 nM EGF for 3 min. They were then fixed and stained with rhodamine phalloidin and viewed with fluorescence microscopy as described in Materials and methods. The total F-actin fluorescence/cell was calculated as the product of the mean fluorescence multiplied by the area in pixels. The data are the means and SEM for a total of 15 cells per condition. The total fluorescence per cell for EGF (5 nM) + cyto D stimulation is significantly different from the other conditions (*t*-test, $P < 10^{-6}$).

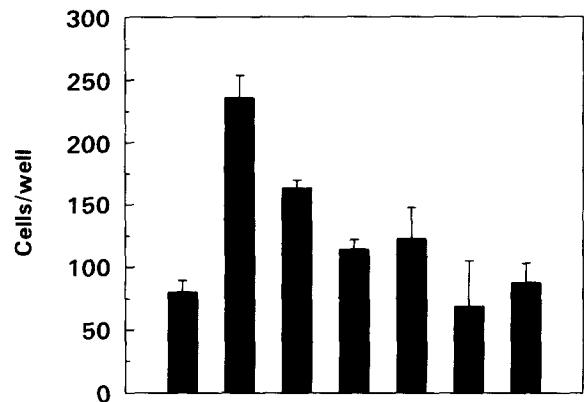


Figure 9. Effects of cytochalasin D on migration in response to EGF. Cells were exposed to buffer or EGF in the bottom well (gradient condition) in the presence of varying amounts of cytochalasin D. After 3 h, the filters were removed and cell migration quantitated as described in Materials and methods. Data are the means and SEM for 12 wells from three separate experiments.

Cells were exposed to buffer or EGF in the bottom well (gradient condition) in the presence of varying amounts of cytochalasin D. After 3 h, the filters were removed and cell migration quantitated as described in Materials and methods. Data are the means and SEM for 12 wells from three separate experiments.

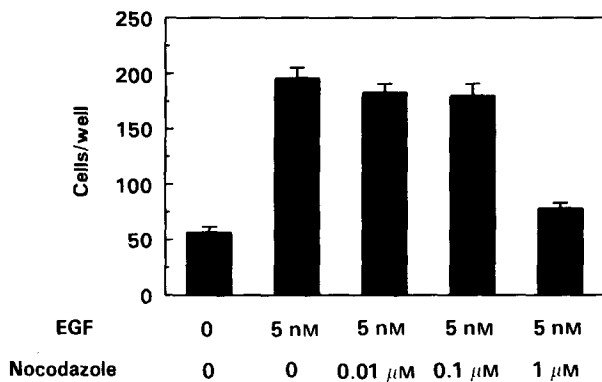


Figure 10. Effects of nocodazole on migration in response to EGF. Cells were exposed to buffer or EGF in the bottom well (gradient condition) in the presence of varying amounts of nocodazole. After 3 h, the filters were removed and cell migration quantitated as described in Materials and methods. Data are the means and SEM for 12 wells from three separate experiments.

reflect the increased time required for the assay compared to the area change: the microchemotaxis assay requires 3 h exposure to cytochalasin, while the area change assay was finished within 5 min of exposure to cytochalasin.

Microtubules might also play a role in responses to EGF. It has been reported that EGF stimulation of MTLn3 cells produces a significant increase in the amount of tubulin present in the cytoskeleton [46]. To test the function of microtubules in chemotaxis and lamellipod extension in response to EGF, we used nocodazole to inhibit microtubule dynamics. Nocodazole (100 nM) was effective in blocking cell division of MTLn3 cells, indicating that the microtubules in MTLn3 cells showed normal sensitivity to nocodazole [47]. However, 100 nM nocodazole had very little effect on chemotaxis to EGF. Higher doses of nocodazole (1 μ M), sufficient to depolymerize the microtubule cytoskeleton, did strongly inhibit chemotaxis (Figure 10). Exposure of cells to 100 nM nocodazole led to a slow reduction in area over 30 min which at least partially recovered after 1 h, while exposure to 1 μ M nocodazole led to a rapid reduction in cell area. However, neither 100 nM nor 1 μ M nocodazole had any effect on EGF-stimulated lamellipod extension (Figure 8).

Discussion

MTLn3 cells demonstrate stimulated lamellipod extensions

There are a number of studies describing the stimulation of tumor cell surface ruffling by EGF.

A431 cells [32,35,46,48,49], KB cells [50], and MCF-7 cells [51] show dramatic increases in cell ruffling and rounding. Application of EGF to NR6 cells expressing EGF receptors results in lamellipodial retraction [52]. Both types of responses are quite distinct from the morphological changes seen with MTLn3 cells. Upon stimulation with EGF, MTLn3 cells flatten and show growth of hyaline lamellipods in parallel with a reduction in ruffling (this report and [46]). Ruffling resumes after the lamellipods begin to retract. There are several possible reasons why different cell types show different motility responses to stimulation of EGF receptors. A431 and KB cells have roughly 10 times more EGF receptors than MTLn3 cells [53–55]. It is possible that the inhibition of growth of A431 and KB cells by EGF is due to the excessive number of EGF receptors [46,56–58]. Similarly, large numbers of stimulated receptors may lead to multiple cycles of actin polymerization and ruffling. Another possibility is that interactions with the extracellular matrix are important. Stimulation with EGF leads to increased adhesivity of MTLn3 cells [46], and reduced adhesivity of A431 cells [40,59]. This interaction with the extracellular matrix may be important in modulating the response. The lamellipods produced by MTLn3 cells are extremely thin and near the substratum, and could rely upon an interaction between extracellular matrix receptors and the substratum. Finally, these differences in response to EGF could correlate with metastatic capability. MTLn3 cells are motile and highly metastatic in spontaneous metastasis assays [38,60], while KB and A431 cells are not used for studying spontaneous metastasis [36,61,62].

EGF-stimulated lamellipod extension is mediated by the EGF receptor

The concentration of EGF that produces a half maximal increase in area, 0.5 nM, lies between the values reported for EGF binding sites on the surface of MTLn3 cells [41]. MTC cells, which show little specific binding of EGF [40], do not respond to the addition of EGF or TGF α with lamellipod extension. This indicates that the responses reported here are mediated by the EGF receptor. There are 10,400 high affinity sites (K_d 0.17 nM), and 46 000 low affinity sites (K_d 1.2 nM) on MTLn3 cells. Since stimulation with 0.2 nM EGF produced only about 25% of the maximal response, and stimulation with 5 nM produced a maximal response, it is possible that the low affinity sites mediate the lamellipod extension.

The dose–response curve for chemotaxis in the microchemotaxis chamber is consistent with results observed with other cell types, with peak responses

occurring in the range of 0.2–2 nm and then decreasing [19–21]. Given that lamellipod extension is a necessary component of cell movement, one might expect that the maximal chemotaxis response should occur near the concentration at which the lamellipod extension (area change) is maximal (5 nm for MTLn3 cells). For most well-characterized chemoattractants, measurements of chemotactic responses using the microchemotaxis chamber show reduced responses occurring at higher concentrations [19–21,63]. The reduction in chemotactic response observed at 25 nm for MTLn3 cells is consistent with this interpretation.

Microtubules are not required for EGF-stimulated lamellipod extension

In contrast to cytochalasin D, nocodazole had relatively little effect on lamellipod expansion. Although 100 nm nocodazole was sufficient to block cell division [47], it was not sufficient to block EGF-induced lamellipod extension or chemotaxis in the microchemotaxis chamber. Nocodazole (1 μ M) did block chemotaxis but did not inhibit EGF-induced lamellipod extension. Chemotactic movement involves a number of additional steps besides extension of a lamellipod. It is possible that microtubule stability is necessary for oriented cell movement while not being necessary for the initial extension of a lamellipod in the direction of higher chemoattractant concentrations.

Actin polymerization is required for EGF-stimulated lamellipod extension

The distribution of F-actin in EGF-induced lamellipods is compatible with actin polymerization playing a key role in their formation. The concentration of F-actin was found to be increased adjacent to the plasma membrane at the leading edge of EGF-induced lamellipods while there was no net change in actin polymer content of cells. Cytochalasin D, a potent inhibitor of barbed end assembly [45], inhibited the accumulation of F-actin at the leading edge, lamellipod extension, and chemotaxis in response to EGF. In addition, cytochalasin D also caused a significant decrease in F-actin content in response to EGF stimulation as compared to its effect on unstimulated cells. These results indicate that EGF stimulates both polymerization at barbed filament ends and depolymerization at pointed filament ends (an event not inhibited by cytochalasin D). As a result, in response to EGF, the content of cellular F-actin in MTLn3 cells remains constant as F-actin polymerizes at the leading edge. Although A431 cells show a net increase in total F-actin [32,35,64,65] in response to EGF, they also show stimulation of both depoly-

merization and polymerization of actin. Depolymerization of stress fibers is mediated by cyclo-oxygenase metabolites, while cortical actin polymerization is produced by lipoxygenase metabolism [32]. These effects may be regulated by the small G proteins rho and rac, as has been shown for fibroblasts [66].

Lamellipod extension could be due to (a) pressure generated by contraction at the rear of the cell, (b) actin–myosin interactions at the leading edge, (c) polymerization of actin at the leading edge, or (d) formation of an actin meshwork followed by osmotic swelling (for reviews see [12,67,68]). The results presented in this paper support models in which actin polymerization generates the force to extend the plasma membrane to produce a lamellipod as in (c) or (d). These models are consistent with cycles of actin polymerization and depolymerization that accompany the extension of pseudopods in chemotactic amoeboid cells after stimulation with chemoattractants [69] and with the behavior of fluorescently-labelled actin filaments in the leading lamella of locomoting keratocytes [70]. A mechanism for polarization of cells in spatial gradients of chemoattractant could include spatial separation of the polymerization and depolymerization processes. If actin polymerization is increased in regions of the cell exposed to higher concentrations of EGF, and actin depolymerization increased in the rest of the cells, the net result would be reorientation of the cell cytoskeleton in the direction of the chemoattractant gradient. This would provide a means for extension of lamellipods towards increased chemoattractant concentrations.

In summary, we have identified a chemoattractant-stimulated extension of lamellipods in a metastatic cell line. Consistent with results obtained with G protein-based signal transduction systems in amoeboid phagocytes such as neutrophils and *Dictyostelium*, our studies indicate that receptor tyrosine kinases also stimulate the production of actin-filled cell extensions. Such extensions occur rapidly after stimulation, and could represent the initial cell response to a chemotactic stimulus. TGF α and the EGF receptor are expressed in normal mammary tissue [71–73] and could mediate normal physiological stimulation of cell motility and proliferation. Such responses might be used by tumor cells during the process of metastasis [40], since the non-metastatic cell line MTC showed little lamellipod extension in response to EGF or TGF α . Alternatively, other chemoattractants, either tissue or tumor derived [74], might utilize lamellipod extension to stimulate cell movement. The proteins that control actin polymerization within these extensions could play key roles in the regulation of the motility of these metastatic cells [75]. Further

work will focus on identifying these proteins, as potentially important regulators of cell motility and metastasis.

Acknowledgements

We gratefully acknowledge many helpful discussions with Garth Nicolson and Rosemarie Lichtner regarding MTLn3 cells. We also thank William Miroff, Jeffrey Wyckoff, Arthur Hayashi, and Scott Staples for valuable assistance. Microscopy was performed in the Image Analysis Facility of the Albert Einstein College of Medicine. J.E.S. was the recipient of a Mellam Family Investigatorship of the New York Heart Association. This research was supported by USAMRDC AIBS 2466, NIHGM25813, NIHGM44246, and NIHGM38511.

References

1. Rosenberg S, 1987, *Surgical Treatment of Metastatic Cancer*. Lippincott: Philadelphia.
2. Fidler IJ and Balch CM, 1987, The biology of cancer metastasis and implications for therapy. *Curr Prob Surg*, **24**, 129–209.
3. Sugarbaker EV, 1979, Cancer metastasis: a product of tumor–host interactions. *Curr Prob Cancer*, **3**, 1–59.
4. Nabi IR, Watanabe H and Raz A, 1992, Autocrine motility factor and its receptor: role in cell locomotion and metastasis. *Cancer Metastasis Rev*, **11**, 5–20.
5. Talmadge JE and Fidler IJ, 1989, Phenotypic heterogeneity and metastasis. In: Sirica AE, ed. *The Pathobiology of Neoplasia*. New York: Plenum Press, pp. 547–72.
6. Lu C and Kerbel RS, 1994, Cytokines, growth factors and the loss of negative growth controls in the progression of human cutaneous malignant melanoma. *Curr Opin Oncol*, **6**, 212–20.
7. Yeatman TJ and Nicolson GL, 1993, Molecular basis of tumor progression: mechanisms of organ-specific tumor metastasis. *Seminars Surg Oncol*, **9**, 256–63.
8. Rinker-Schaeffer CW, Partin AW, Isaacs WB, et al. 1994, Molecular and cellular changes associated with the acquisition of metastatic ability by prostatic cancer cells. *Prostate*, **25**, 249–265.
9. Monsky WL and Chen WT, 1993, Proteases of cell adhesion proteins in cancer. *Seminars Cancer Biol*, **4**, 251–8.
10. Aznavoorian S, Murphy AN, Stetler-Stevenson WG, et al. 1993, Molecular aspects of tumor cell invasion and metastasis. *Cancer*, **71**, 1368–83.
11. Jones JG, Segall J and Condeelis J, 1991, Molecular analysis of amoeboid chemotaxis: parallel observations in amoeboid phagocytes and metastatic tumor cells. *Experientia Suppl*, **59**, 1–16.
12. Condeelis J, 1993, Life at the leading edge: the formation of cell protrusion. *Ann Rev Cell Biol*, **9**, 411–44.
13. Devreotes PN and Zigmond SH, 1988, Chemotaxis in eukaryotic cells: a focus on leukocytes and *Dictyostelium*. *Ann Rev Cell Biol*, **4**, 649–86.
14. Silletti S and Raz A, 1993, Autocrine motility factor is a growth factor. *Biochem Biophys Res Commun*, **194**, 446–57.
15. Stracke M, Liotta LA and Schiffmann E, 1993, The role of autotaxin and other motility stimulating factors in the regulation of tumor cell motility. *Symp Soc Exp Biol*, **47**, 197–214.
16. Hoelting T, Siperstein AE, Clark OH, et al. 1994, Epidermal growth factor enhances proliferation, migration, and invasion of follicular and papillary thyroid cancer *in vitro* and *in vivo*. *J Clin Endocr Metab*, **79**, 401–8.
17. Pedersen PH, Ness GO, Engebraaten O, et al. 1994, Heterogeneous response to the growth factors [EGF, PDGF (bb), TGF-alpha, bFGF, IL-2] on glioma spheroid growth, migration and invasion. *Int J Cancer*, **56**, 255–61.
18. Wang X, Kamiyama K, Iguchi I, et al. 1994, Enhancement of fibronectin-induced migration of corneal epithelial cells by cytokines. *Invest Ophthalmol Vis Sci*, **35**, 4001–7.
19. Royce LS and Baum BJ, 1991, Physiologic levels of salivary epidermal growth factor stimulate migration of an oral epithelial cell line. *Biochim Biophys Acta*, **1092**, 401–3.
20. Grotendorst GR, Soma Y, Takehara K, et al. 1989, EGF and TGF-alpha are potent chemoattractants for endothelial cells and EGF-like peptides are present at sites of tissue regeneration. *J Cell Physiol*, **139**, 617–23.
21. Blay J and Brown KD, 1985, Epidermal growth factor promotes the chemotactic migration of cultured rat intestinal epithelial cells. *J Cell Physiol*, **124**, 107–12.
22. Kundra V, Escobedo JA, Kazlauskas A, et al. 1994, Regulation of chemotaxis by the platelet-derived growth factor receptor-beta. *Nature*, **367**, 474–6.
23. Yenush L, Kundra V, White MF, et al. 1994, Functional domains of the insulin receptor responsible for chemotactic signaling. *J Biol Chem*, **269**, 100–4.
24. Li Y, Bhargava MM, Joseph A, et al. 1994, Effect of hepatocyte growth factor/scatter factor and other growth factors on motility and morphology of non-tumorigenic and tumor cells. *In Vitro Cell Devel Biol An*, **30A**, 105–10.
25. Gherardi E, Sharpe M, Lane K, et al. 1993, Hepatocyte growth factor/scatter factor (HGF/SF), the *c-met* receptor and the behaviour of epithelial cells. *Symp Soc Exp Biol*, **47**, 163–81.
26. Khazaie K, Schirrmacher V and Lichtner RB, 1993, EGF receptor in neoplasia and metastasis. *Cancer Metastasis Rev*, **12**, 255–74.
27. Weidner N and Gasparini G, 1994, Determination of epidermal growth factor receptor provides additional prognostic information to measuring tumor angiogenesis in breast carcinoma patients. *Breast Canc Res Treat*, **29**, 97–107.
28. Fox SB, Smith K, Hollyer J, et al. 1994, The epidermal growth factor receptor as a prognostic marker: results of 370 patients and review of 3009 patients. *Breast Canc Res Treat*, **29**, 41–9.
29. Veale D, Kerr N, Gibson GJ, et al. 1993, The relationship of quantitative epidermal growth factor receptor expression in non-small cell lung cancer to long term survival. *Br J Cancer*, **68**, 162–5.
30. Mayer A, Takimoto M, Fritz E, et al. 1993, The prognostic significance of proliferating cell nuclear

- antigen, epidermal growth factor receptor, and *mdr* gene expression in colorectal cancer. *Cancer*, **71**, 2454–60.
31. Itakura Y, Sasano H, Shiga C, *et al.* 1994, Epidermal growth factor receptor overexpression in esophageal carcinoma. An immunohistochemical study correlated with clinicopathologic findings and DNA amplification. *Cancer*, **74**, 795–804.
 32. Peppelenbosch MP, Tertoolen LG, Hage WJ, *et al.* 1993, Epidermal growth factor-induced actin remodeling is regulated by 5-lipoxygenase and cyclooxygenase products. *Cell*, **74**, 565–75.
 33. Kuppuswamy D and Pike LJ, 1991, Desensitization of the EGF receptor alters its ability to undergo EGF-induced dimerization. *Cell Signalling*, **3**, 107–17.
 34. Osherov N and Levitzki A, 1994, Epidermal-growth-factor-dependent activation of the *src*-family kinases. *Eur J Biochem*, **225**, 1047–53.
 35. Dadabay CY, Patton E, Cooper JA, *et al.* 1991, Lack of correlation between changes in polyphosphoinositide levels and actin/gelsolin complexes in A431 cells treated with epidermal growth factor. *J Cell Biol*, **112**, 1151–6.
 36. Price JE, Sauder DN and Fidler IJ, 1988, Tumorigenicity and metastatic behavior in nude mice of two human squamous cell carcinoma lines that differ in production of the cytokine ETAF/IL-1. *J Invest Dermatol*, **91**, 258–62.
 37. Neri A, Welch D, Kawaguchi T, *et al.* 1982, Development and biologic properties of malignant cell sublines and clones of a spontaneously metastasizing rat mammary adenocarcinoma. *J Natl Cancer Inst*, **68**, 507–17.
 38. Welch DR, Neri A and Nicolson GL, 1983, Comparison of 'spontaneous' and 'experimental' metastasis using rat 13762 mammary adenocarcinoma metastatic cell clones. *Invasion Metastasis*, **3**, 65–80.
 39. Welch DR, Krizman DB and Nicolson GL, 1984, Multiple phenotypic divergence of mammary adenocarcinoma cell lines. I. *In vitro* and *in vivo* properties. *Clin Exp Metastasis*, **2**, 333–55.
 40. Kaufmann AM, Khazaie K, Wiedemuth M, *et al.* 1994, Expression of epidermal growth factor receptor correlates with metastatic potential of 13762NF rat mammary adenocarcinoma cells. *Int J Oncol*, **4**, 1149–55.
 41. Lichtner RB, Wiedemuth M, Kittmann A, *et al.* 1992, Ligand-induced activation of epidermal growth factor receptor in intact rat mammary adenocarcinoma cells without detectable receptor phosphorylation. *J Biol Chem*, **267**, 11872–80.
 42. McKenna NM and Wang YL, 1989, Culturing cells on the microscope stage. *Meth Cell Biol*, **29**, 195–205.
 43. Soll DR, 1988, 'DMS,' a computer-assisted system for quantitating motility, the dynamics of cytoplasmic flow, and pseudopod formation: its application to *Dictyostelium* chemotaxis. *Cell Motil Cytoskeleton*, **10**, 91–106.
 44. Condeelis J and Hall AL, 1991, Measurement of actin polymerization and cross-linking in agonist-stimulated cells. *Meth Enzymol*, **196**, 486–96.
 45. Sampath P and Pollard TD, 1991, Effects of cytochalasin, phalloidin, and pH on the elongation of actin filaments. *Biochemistry*, **19**, 1973–80.
 46. Lichtner RB, Wiedemuth M, Noeske-Jungblut C, *et al.* 1993, Rapid effects of EGF on cytoskeletal structures and adhesive properties of highly metastatic rat mammary adenocarcinoma cells. *Clin Exp Metastasis*, **11**, 113–25.
 47. Jordan MA, Thrower D and Wilson L, 1992, Effects of vinblastine, podophyllotoxin and nocodazole on mitotic spindles. Implications for the role of microtubule dynamics in mitosis. *J Cell Sci*, **102**, 401–16.
 48. Chinkers M, McKanna JA and Cohen S, 1981, Rapid rounding of human epidermoid carcinoma cells A-431 induced by epidermal growth factor. *J Cell Biol*, **88**, 422–9.
 49. Chinkers M, McKanna JA and Cohen S, 1979, Rapid induction of morphological changes in human carcinoma cells A-431 by epidermal growth factor. *J Cell Biol*, **83**, 260–5.
 50. Miyata Y, Nishida E and Sakai H, 1988, Growth factor- and phorbol ester-induced changes in cell morphology analyzed by digital image processing. *Exp Cell Res*, **175**, 286–97.
 51. van Larebeke NA, Bracke ME and Mareel MM, 1992, Simple method for quantification of fast plasma membrane movements. *Cytometry*, **13**, 1–8.
 52. Welsh JB, Gill GN, Rosenfeld MG, *et al.* 1991, A negative feedback loop attenuates EGF-induced morphological changes. *J Cell Biol*, **114**, 533–43.
 53. Kadowaki T, Koyasu S, Nishida E, *et al.* 1986, Insulin-like growth factors, insulin, and epidermal growth factor cause rapid cytoskeletal reorganization in KB cells. Clarification of the roles of type I insulin-like growth factor receptors and insulin receptors. *J Biol Chem*, **261**, 16141–7.
 54. Wrann MM and Fox CF, 1979, Identification of epidermal growth factor receptors in a hyperproducing human epidermoid carcinoma cell line. *J Biol Chem*, **254**, 8083–6.
 55. Lichtner RB and Schirmacher V, 1990, Cellular distribution and biological activity of epidermal growth factor receptors in A431 cells are influenced by cell–cell contact. *J Cell Physiol*, **144**, 303–12.
 56. Koyasu S, Kadowaki T, Nishida E, *et al.* 1988, Alteration in growth, morphology, and cytoskeletal structures of KB cells induced by epidermal growth factor and transforming growth factor-beta. *Exp Cell Res*, **176**, 107–16.
 57. Gill GN and Lazar CS, 1981, Increased phosphotyrosine content and inhibition of proliferation in EGF-treated A431 cells. *Nature*, **293**, 305–7.
 58. Kawamoto T, Sato JD, Le A, *et al.* 1983, Growth stimulation of A431 cells by epidermal growth factor: identification of high-affinity receptors for epidermal growth factor by an anti-receptor monoclonal antibody. *Proc Natl Acad Sci USA*, **80**, 1337–41.
 59. Rieber M, Castillo MA, Rieber MS, *et al.* 1988, Decrease in tumor-cell attachment and in a 140-kDa fibronectin receptor correlate with greater expression of multiple 34-kDa surface proteins and cytoplasmic 54-kDa components. *Int J Cancer*, **41**, 96–100.
 60. Nakajima M, Welch DR, Wynn DM, *et al.* 1993, Serum and plasma M(r) 92,000 progelatinase levels correlate with spontaneous metastasis of rat 13762NF mammary adenocarcinoma. *Cancer Res*, **53**, 5802–7.
 61. Schechter B, Arnon R, Wilchek M, *et al.* 1991, Indirect immunotargeting of cis-Pt to human epidermoid carcinoma KB using the avidin–biotin system. *Int J Cancer*, **48**, 167–72.

62. Aboud-Pirak E, Hurwitz E, Pirak ME, et al. 1988, Efficacy of antibodies to epidermal growth factor receptor against KB carcinoma *in vitro* and in nude mice. *J Natl Cancer Inst*, **80**, 1605–11.
63. Harvath L, Falk W and Leonard EJ, 1980, Rapid quantitation of neutrophil chemotaxis: use of a polyvinylpyrrolidone-free polycarbonate membrane in a multiwell assembly. *J Immunol Meth*, **37**, 39–45.
64. Rijken PJ, Hage WJ, van Bergen en Henegouwen PM, et al. 1991, Epidermal growth factor induces rapid reorganization of the actin microfilament system in human A431 cells. *J Cell Sci*, **100**, 491–9.
65. Schlessinger J and Geiger B, 1981, Epidermal growth factor induces redistribution of actin and alpha-actinin in human epidermal carcinoma cells. *Exp Cell Res*, **134**, 273–9.
66. Ridley AJ, 1994, Membrane ruffling and signal transduction. *Bioessays*, **16**, 321–7.
67. Oster G and Perelson A, 1987, The physics of cell motility. *J Cell Sci*, **8**, 35–54.
68. Egelhoff TT and Spudich JA, 1991, Molecular genetics of cell migration: *Dictyostelium* as a model system. *Trends Genetics*, **7**, 161–6.
69. Hall AL, Warren V, Dharmawardhane S, et al. 1989, Identification of actin nucleation activity and polymerization inhibitor in ameboid cells: their regulation by chemotactic stimulation. *J Cell Biol*, **109**, 2207–13.
70. Theriot JA and Mitchison TJ, 1992, Comparison of actin and cell surface dynamics in motile fibroblasts. *J Cell Biol*, **119**, 367–77.
71. Bates SE, Valverius EM, Ennis BW, et al. 1990, Expression of the transforming growth factor-alpha/epidermal growth factor receptor pathway in normal human breast epithelial cells. *Endocrinology*, **126**, 596–607.
72. Coleman S, Silberstein GB and Daniel CW, 1988, Ductal morphogenesis in the mouse mammary gland: evidence supporting a role for epidermal growth factor. *Develop Biol*, **127**, 304–15.
73. Snedeker SM, Brown CF and DiAugustine RP, 1991, Expression and functional properties of transforming growth factor alpha and epidermal growth factor during mouse mammary gland ductal morphogenesis. *Proc Natl Acad Sci USA*, **88**, 276–80.
74. Atnip KD, Carter LM, Nicolson GL, et al. 1987, Chemotactic response of rat mammary adenocarcinoma cell clones to tumor-derived cytokines. *Biochem Biophys Res Commun*, **146**, 996–1002.
75. Cunningham CC, 1992, Actin structural proteins in cell motility. *Cancer Metastasis Rev*, **11**, 69–77.